The Determination of the "Flat-band" Potential of Nitrogen-stabilized n-TiO_2 Photoanode

Taketsugu HIRAI,* Isao TARI, and Tsutomu OHZUKU
Department of Synthetic Chemistry, Faculty of Engineering, Okayama University, Tsushima, Okayama 700
(Received March 28, 1980)

The differential capacitance (C) and the photocurrent onset voltage (E_p) of nitrogen-stabilized n-TiO_2 semiconductor electrodes were measured in buffered Na_3PO_4 solutions. The C^{-2} *vs.* E plots did not show the Mott-Schottky (MS) behavior. In order to explain the nonlinearity in MS plots, the distribution in donor density (N_d) at the solid side and the contribution of the electrical double layer at the solution side to the total capacitance were considered. The characterized flat-band potential (E_{fb}) and the zero-charge potential (E_{zc}) were defined from the derived equations. The roles of the defined E_{fb} and E_{zc} in the photocurrent onset voltage (E_p) were also considered, and the reason why E_p differed from E_{fb} was explained using the "Gate" model.

In semiconductor electrochemistry, the determinations of both the flat-band potential and the charge carrier density are important, for they are the basic parameters of semiconductor electrodes. These quantities can be determined by the Mott-Schottky relationship from the measurement of the differential capacitance. However, the experimental results which have been reported for single and polycrystalline semiconductor electrodes usually show some deviations from ideality.[1-6] The possible sources of such deviation from ideality have been discussed by several authors.[1,4,7-9] One of these treatments, that by De Gryse *et al.*,[7] is a quantitative one. They derived another expression by considering the effect of the Helmholtz layer at the semiconductor/electrolyte interface. However, the C^{-2} *vs.* E plots do not allow the E_{fb} values to be determined unless the Helmholtz layer capacitance is known, even when the experimental C^{-2} *vs.* E plot is a straight line.

Our differential capacitance data for nitrogen-stabilized n-TiO_2 semiconductor electrodes, to be reported here, do not show the Mott-Schottky behavior. The objective of this report is to understand the capacitance data, together with the photoelectrochemical property, and to discuss the uncertainty in the determination of the flat-band potential.

Experimental

The nitrogen-stabilized n-type semiconductor ($TiN_{0.07}O_{1.93}$) electrode, which had been proved to be highly resistive to photocorrosions, was the same as that described in a previous paper.[12]

The cell impedance between the $TiN_{0.07}O_{1.93}$ electrode and a far larger platinum electrode was measured by means of an impedance bridge, type DRZ-1 (Ando Electric Corp.), with an audio oscillator, type 4200-A (Yokogawa-Hewlett-Packard), and a tuned null detector, type 4403-A (Yokogawa-Hewlett-Packard). The absolute values of the impedance $|z|$ and the phase angle, θ, as functions of the bias voltage (*vs.* SCE) were measured at 0.3—10 kHz. The electrolytes used were 0.1 M Na_3PO_4 aqueous solutions, adjusted their pHs with a concd NaOH or H_3PO_4 solution.

The anodic photocurrent was measured in the usual manner under full illumination by a 500-W xenon arc lamp at room temperature.

Results

Differential Capacitance Measurements. Figure 1 shows the differential capacitance at 500 Hz as a function of the electrode potential for the $TiN_{0.07}O_{1.93}$ electrode in several buffered Na_3PO_4 solutions. All the C *vs.* E curves showed their peaks in the cathodic region. Although the capacitance values varied somewhat, thus showing the frequency dispersion, a similar trend was usually observed in the frequency range of 0.3—10 kHz.

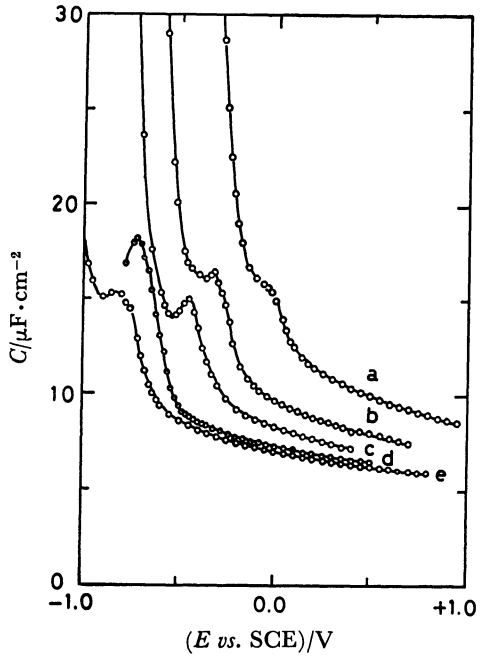

Fig. 1. C *vs.* E curves for $TiN_{0.07}O_{1.93}$ electrode in 0.1 M Na_3PO_4 solutions.
pH; (a): 1.0, (b): 5.0, (c): 7.0, (d): 10.0, (e): 12.0.

In order to determine the basic parameters for this electrode, the C^{-2} *vs.* E plots were applied. According to the Mott-Schottky relationship, the C^{-2} *vs.* E plots should give a straight line over a wide range of potentials. However, the experimental results in Fig. 2 do not show an ideal MS-behavior, so the E_{fb} and N_d values could not be determined.

Photocurrent Onset Voltage. The anodic photo-

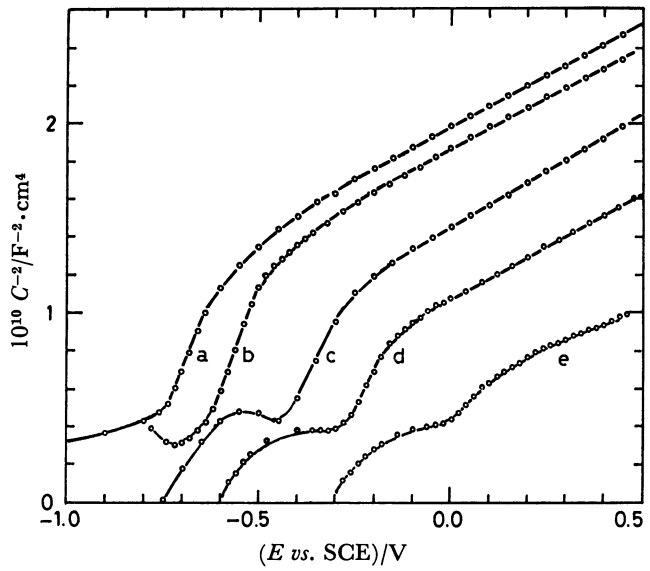

Fig. 2. C^{-2} *vs.* E plots of $TiN_{0.07}O_{1.93}$ electrode in 0.1 M Na_3PO_4 buffered solutions.
pH; (a): 12.0, (b): 10.0, (c): 7.0, (d): 5.0, (e): 1.0.

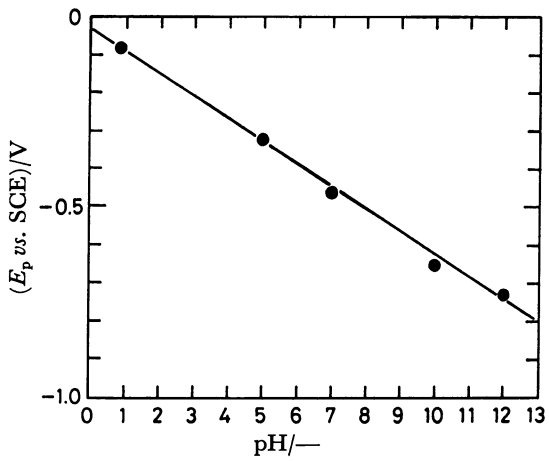

Fig. 3. The pH dependence of the anodic photocurrent onset voltage E_p.

current onset voltage (E_p) against the solution pH is plotted in Fig. 3. The anodic photocurrent onset voltage showed a linear dependence on pH, which can be represented by:

$$E_p = -0.04 - 0.06\ \text{pH}\ (vs.\ \text{SCE}).$$

Discussion

Differential Capacitance at the Semiconductor/Electrolyte Interface. In order to elucidate the nonlinearity in C^{-2} *vs.* E plots, we considered the possible sources of effects on the total capacitance. The whole differential capacity (C) across the semiconductor/electrolyte interface is represented by:

$$1/C = 1/C_{sc} + 1/C_d + 1/C_c, \quad (1)$$

where C_{sc}, C_d, and C_c indicate the capacitance of the space charge layer, the diffused double layer, and the compact double layer respectively. Some investigators omit the $1/C_d$ and/or $1/C_c$ terms in Eq. 1 when the ionic strength is fairly large. The $1/C_d+1/C_c$ term, however, cannot be omitted, especially when the potential drop across the space charge layer is nearly equal to zero, because the condition of $1/C_{sc} \gg 1/C_d + 1/C_c$ does not hold.

The C_{sc} as a function of the potential is usually represented by MS's equation. However, the practical experimental conditions seem to be far from the given conditions of MS assumptions. Among them, the assumptions concerning donor density, which is independent of the distance from the semiconductor surface and the absence of an interfacial layer, such as an insulating layer, are not fulfilled in many real cases for semiconductors exposed to an electrolyte. The semiconductor surface in contact with an electrolyte has, more or less, interfacial layers, which may be formed by a chemical reoxidation or an ion-exchange reaction, because one is a solid electric conductor, and another is a liquid ionic conductor. Therefore, the donor density at the semiconductor surface must be zero, and the distribution in the donor density is developed in the direction perpendicular to the surface. Such situations seem to be readily formed in the case of heavily doped semiconductors,[1,2] as in our case, and the ideal linearity in C^{-2} *vs.* E plots is not to be expected.

As has been stated above, we presume the distribution in donor density, N_d, to be:

$$N_d = ax, \quad (2)$$

where a is a distribution coefficient in cm^{-4} and where x is a distance in cm.

The corresponding boundary conditions are:

$$\phi = \Delta\phi_{sc} - \frac{kT}{e} \text{ at } x = 0, \quad (3)$$

$$\frac{d\phi}{dx} = 0,\ \phi = 0 \text{ at } x = d, \quad (4)$$

in which kT/e indicates the volts of the equivalent thermal energy. By solving Poisson's equation under the given boundary conditions, we obtain:

$$C_{sc}^{-3} = \left(\frac{3}{\varepsilon^2\varepsilon_0^2 ea}\right)\left(\Delta\phi_{sc} - \frac{\kappa T}{e}\right), \quad (5)$$

where ε and ε_0 are the dielectric constants of the semiconductor and the vacuum respectively and where e is an electron charge. The $\Delta\phi_{sc}$ is related to an electrode potential by:

$$\Delta\phi_{sc} = E - E_{fb}. \quad (6)$$

E_{fb} is the flat-band potential at which the electric field is reversed in the depletion layer.

From Eq. 1, we define the capacity, C_e, as:

$$1/C_e = 1/C_d + 1/C_c. \quad (7)$$

The dependence of C_e on the potential is represented by:

$$C_e = C_0 + b(E - E_{zc})^2. \quad (8)$$

C_0 is a minimum capacity, and E_{zc} is the zero-charge potential where the charge in the diffused double layer is reduced to zero. Equation 8 is a phenomelogical equation analogous to the electrical double-layer theory for mercury electrodes.[10]

Equations 5, 7, and 8 give the whole representation

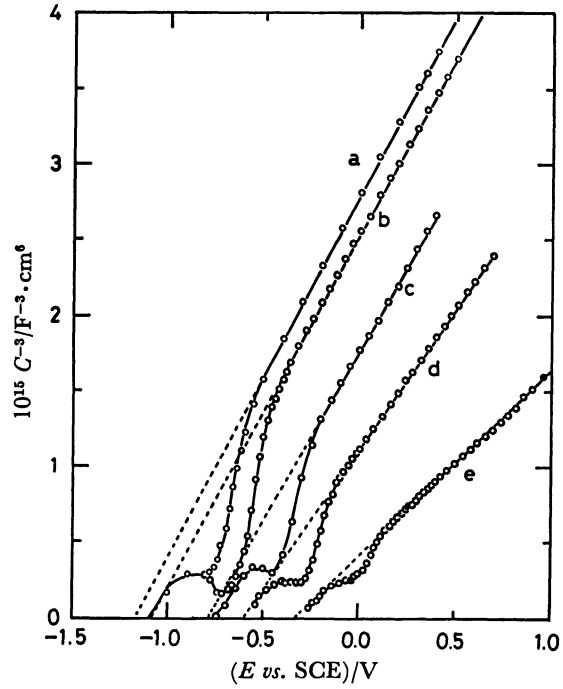

Fig. 4. C^{-3} *vs.* E plots of $TiN_{0.07}O_{1.93}$electrode in 0.1 M Na_3PO_4 buffered solutions.
pH; (a) 12.0 (b) 10.0 (c) 7.0 (d) 5.0 (e) 1.0.

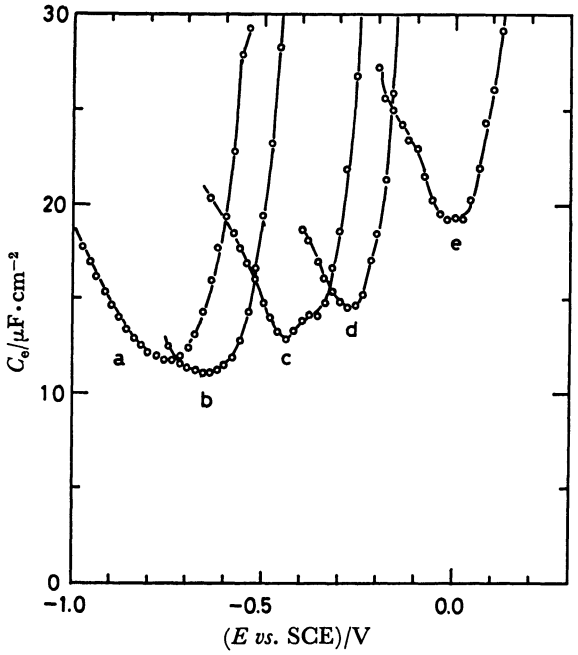

Fig. 5. C_e *vs.* E plots of $TiN_{0.07}O_{1.93}$ electrode in 0.1 M Na_3PO_4 buffered solutions.
pH; (a): 12.0, (b): 10.0, (c) 7.0, (d): 5.0, (e): 1.0.

of the differential capacity across the semiconductor/electrolyte interface as function of the electrode potential.

In order to check the validity of the above treatment, the original experimental results in Fig. 1 are replotted as Fig. 4. As predicted by Eq. 5, straight lines over adequate range of applied potentials are obtained in the C^{-3} *vs.* E plots when $C_e \gg C_{sc}$. In the region of $C_e < C_{sc}$, a distinct deviation from the straight line is observed. From Eq. 1, such a deviation can be said to be caused by the C_e component. The C_e values calculated from Eq. 1 are shown in Fig. 5. The C_e *vs.* E plots obey the parabolic relationship of Eq. 8. Consequentry, the presumptions of Eqs. 2 and 8 are valid in this case.

From the above considerations, we can determine the E_{fb}, E_{zc}, and a values in Eq. 5 as basic parameters of the semiconductor electrode in contact with an electrolyte.

Photocurrent Onset Voltage. It is said that the anodic photocurrent begins to flow at the "flat-band" potential in the case of an n-type semiconductor system.[11] This is the reason why the "flat-band" potential can be determined by measuring the E_p values, even when the capacitance measurement is not attainable. However, it is questionable whether the true E_{fb} values are thus obtained. In order to illustrate this, we compared the characterized E_{fb} and E_{zc} values with the E_p values in Table 1. E_{fb}, as defined by Eq. 5, is obtained by extrapolating to $C^{-3}=0$ in Fig. 4, while E_{zc}, as defined by Eq. 8, is obtained from the minimum of the C *vs.* E plots in Fig. 5.

Table 1. Comparison of E_{fb}, E_{zc}, and E_p values for several pH's of solutions

pH	E_{fb} *vs.* SCE / V	E_{zc} *vs.* SCE / V	E_p *vs.* SCE / V
1.0	−0.41±0.02	−0.02±0.03	−0.08±0.02
5.0	−0.57	−0.28	−0.32
7.0	−0.76	−0.44	−0.46
10.0	−1.07	−0.65	−0.65
12.0	−1.14	−0.75	−0.73

As is shown in Table 1, the E_{fb} values do not agree with the E_p values, which are usually more anodic than the E_{fb} values. However, the E_p values agree with the E_{zc} values within the limits of experimental error. This indicates that the anodic photocurrent begins to flow not at the flat-band potential, but at the zero-charge potential. In order to understand how the anodic photocurrent is allowed to pass across the semiconductor/electrolyte interface, and to find the reason why the photocurrent onset voltage differs from the flat-band potential, the following "Gate" model is proposed.

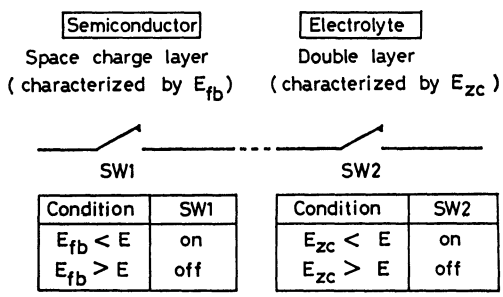

Fig. 6. "Gate" model for an explanation of the photocurrent onset voltage related to E_{fb} and E_{zc} in the case of N-type semiconductor electrode in contact with an electrolyte solution.

SW1 and SW2 in Fig. 6 behave like "Gate" because of its field effect, connected with holes and related ions for an n-type semiconductor electrode in contact with an electrolyte solution. If the condition of $E_{fb}<E_{zc}$ holds, the E_p value should be equal to the E_{zc} value. This is because the hole is permited to migrate to the semiconductor surface, *i.e.*, SW1 is closed, in the potential range of $E_{fb}<E$, but the mass transfer of the related ions is forbidden until E is more positive than E_{zc}, *i.e.*, SW2 is opened. Conversely, the E_p value should be equal to the E_{fb} value when $E_{fb}>E_{zc}$. By considering the "Gate" model, we could explain why the E_p value differed from the E_{fb} value.

We feel that all the semiconductors in contact with an electrolyte solution have the basic parameters of E_{fb} and E_{zc}. Such behavior was also observed for the reduced rutile single crystal and the CVD-TiO_2 semiconductor electrode. Recently, the existence of the surface state has been reported.[13-17] However, the argument of the surface state is not dealt with in this study. We think its capacitance probably contains the measured C_e value. From the above considerations, it can be emphasized that the determination of E_{fb} by E_p measurements has the possibility of being misleading as to the E_{fb} value.

Conclusion

We could give an explanation of the possible sources of deviation from the Mott-Schottky behavior of the nitrogen-stabilized TiO_2 semiconducting electrode, and point out some problems in the determination of the "flat-band" potential. The distribution of the donor density, N_d, in the direction perpendicular to the semiconductor surface and the contribution of the double layer to the total capacity caused the non-linearity in C^{-2} *vs.* E plots. When the distributed donor density is represented by $N_d=ax$, the C^{-3} *vs.* E plots are linear instead of the C^{-2} *vs.* E plots. The remaining capacitive component, C_e, in C^{-3} *vs.* E is proved to be an effect of the double-layer capacity by showing the C_e *vs.* E plots, which are characterized by their E_{zc} values.

In order to understand the roles of E_{fb} and E_{zc} in photoelectrochemical effect, the "Gate" model was proposed. By using the "Gate" model, which was characterized by both the E_{fb} and E_{zc} values for an n-type semiconductor electrode in contact with an electrolyte solution, we explained why the photocurrent onset, E_p, differed from E_{fb}. Moreover, a warning on the determination of the flat-band potential from the photocurrent onset voltage measurement was given.

Although the essential problems concerned with the semiconductor/electrolyte interface remain, we could partly elucidate the complicated behavior of a semiconductor electrode in contact with an electrolyte solution.

The present work was supported by a Grant-in-Aid for Energy Research No. 505035 from the Ministry of Education, Science and Culture.

References

1) D. M. Tench and E. Yeager, *J. Electrochem. Soc.*, **120**, 164 (1973).
2) R. H. Wilson, L. A. Harris, and M. E. Gerstner, *J. Electrochem. Soc.*, **126**, 844, 850 (1979).
3) A. Fujishima, A. Sakamoto, and K. Honda, *Seisan Kenkyu*, **21**, 450 (1969).
4) J. H. Kennedy and K. W. Frese, Jr., *J. Electrochem. Soc.*, **125**, 723 (1978).
5) J. S. Curran and W. Gissler, *J. Electrochem. Soc.*, **126**, 56 (1979).
6) R. A. Fredlein and A. J. Bard, *J. Electrochem. Soc.*, **126**, 1892 (1979).
7) R. De Gryse, W. P. Gomes, F. Cordon, and J. Vennik, *J. Electrochem. Soc.*, **122**, 711 (1975).
8) M. Tomkiewicz, *J. Electrochem. Soc.*, **126**, 1505 (1979).
9) F. Cordon and W. P. Gomes, *J. Phys. D.*, **11**, L63 (1978).
10) P. Delahay, in "Double-layer and Electrode Kinetics," John Wiley & Sons, New York (1965), Chaps. 3 and 5.
11) H. H. Kung, H. S. Jarrett, A. W. Sleight, and A. Ferretti, *J. Appl. Phys.*, **48**, 2463 (1977).
12) T. Hirai, I. Tari, and J. Yamura, *Bull. Chem. Soc. Jpn.*, **51**, 3057 (1978).
13) V. E. Henrich, G. Dresselhaus, and H. J. Zeiger, *Phys. Rev. Lett.*, **36**, 1335 (1976).
14) V. E. Henrich, G. Dresselhaus, and H. J. Zeiger, *Solid State Commun.*, **24**, 623 (1977).
15) W. J. Lo, Y. W. Chung, and G. A. Somorjai, *Surf. Sci.*, **71** 199 (1978).
16) W. J. Lo and G. A. Somorjai, *Phys. Rev. B*, **17**, 4942 (1978).
17) V. E. Henrich, G. Dresselhaus, and H. J. Zeiger, *Phys. Rev. B*, **17**, 4908 (1978).